

PROPERTIES OF TRANSITION- AND SYNCHROTRON RADIATION AT FLUTE

M. Schwarz*, A.-S. Müller, KIT, Karlsruhe, Germany
 M. Schmelling, MPIK, Heidelberg, Germany

Abstract

FLUTE (Fermi-infrarot Linac Und Test Experiment) is a 41 MeV linear accelerator currently under construction at KIT. It is aimed at accelerator physics and THz radiation research. For this reason the machine will cover a wide range of bunch charges (1 pC up to 3 nC) and lengths (1 fs to 300 fs). One aim of FLUTE is the study of different mechanisms for the generation of intense THz pulses, such as transition- (TR) or synchrotron radiation (SR). In this contribution, we calculate and compare various pulse properties, such as spectra, and electric fields, for both TR and SR.

MOTIVATION

Coherent radiation is emitted by electron bunches whenever the wavelength in question is larger than the bunch length. The test facility FLUTE [1] aims to produce bunches with charges 1 pC and bunch lengths 1 fs. In this paper, we compare our own semi-analytic methods for calculating the electric field of a coherent THz pulse [2] with analytic results and standard numerical methods. Next, we apply it to compute the electric field pulse of a simulated bunch profile for synchrotron- (SR) and transition radiation (TR).

RADIATION FROM ULTRA-SHORT BUNCHES

A bunch consists of N particles at positions t_i . Assuming that each particle emits a pulse with electric field $E_0(t)$ the field of the entire bunch is given by the superposition of the individual pulses

$$E(t) = \sum_{i=0}^{N-1} E_0(t - t_i).$$

Here, we are only interested in the coherent field, and thus, ignoring the transverse bunch size, approximate the bunch by a continuous normalized longitudinal density $\rho(t)$. The field of the pulse is then a convolution of the single particle pulse $E_0(t)$ and the bunch profile $\rho(t)$

$$E(t) = \int_{-\infty}^{\infty} E_0(t - \tau) \rho(\tau) d\tau.$$

It is more convenient to solve the convolution in the frequency domain

$$\varepsilon(t) \equiv \int_0^{\infty} \tilde{E}_0(\omega) \tilde{\rho}(\omega) e^{-i\omega t} d\omega, \quad (1a)$$

$$E(t) = N \operatorname{Re} \left[e^{-i\phi} \varepsilon(t) \right]. \quad (1b)$$

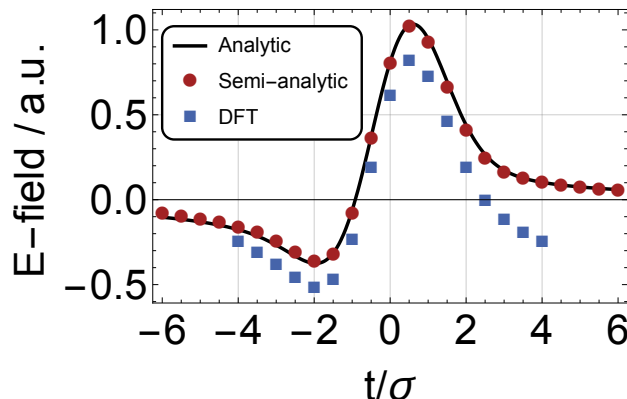


Figure 1: Electric field of a synchrotron radiation pulse emitted by a Gaussian bunch, calculated according to Eq. (1). Eq. (1) was solved analytically (continuous curve) [3], employing the discrete Fourier transform (DFT, boxes), and our own semi-analytic code (circles) [2]. Compared to the analytic result, the DFT method yields both a wrong peak field and pulse shape.

Here and in the following, a \sim above a symbol denotes its representation in the frequency domain. The phase ϕ is a property of the emission process, and determines whether the pulse is single or "half" cycle. Setting $\phi = 0, 180^\circ$ yields a "half" cycle pulse whereas $\phi = \pm 45$ or $\pm 135^\circ$ leads to a single cycle pulse.

The main problem is to solve Eq. (1a) for different spectra \tilde{E}_0 and general bunch profiles ρ . A standard way of computing the convolution would be to sample the bunch profile at reasonably many points, and use the discrete Fourier transform (DFT) to both obtain $\tilde{\rho}$ and subsequently compute Eq. (1a). That this procedure only asymptotically, i.e. for many sampling points and a large time interval, yields the correct result is demonstrated in Fig. 1 for a Gaussian bunch emitting low-frequency synchrotron radiation, $\tilde{E}_0(\omega) \sim \omega^{1/6}$. To apply the DFT, the profile was sampled by 17 equidistant data points in the interval $[-4\sigma, 4\sigma]$, containing more than 99.9% of the bunch. The boxes in Fig. 1 depict the result obtained by using the DFT. Notice that it is limited to times given by the sampling interval. The continuous curve shows the analytic result [3]. Here, the DFT gives a peak field that is about 22% too low, and the wrong shape at large (positive) times¹.

One reason for the discrepancy is that the integral $\int_{-\infty}^{\infty} E(t) dt$ needs to vanish [4]. Thus, a positive peak needs to be balanced by a negative tail. The analytic calculation is

¹ An agreement better than 1% requires a sampling interval $\pm 50\sigma$ and ten times as many data points.

* markus.schwarz@kit.edu

not limited to any finite time interval, and can thus balance a short positive peak by a large negative tail. However, the DFT is periodic in time, limiting the time interval in which to bring the integral to zero. Thus, the peak field is not as large compared to the true analytic result, and its positive value must be compensated by a strong negative tail.

For a limited number of spectral shapes $\tilde{E}_0(\omega)$ it is possible to solve Eq. (1a) analytically for general bunch profiles by interpolating the profile [3]. But for both general profiles and arbitrary spectra, one must resort to numerical approaches. In [2] we presented a fast semi-analytic algorithm that is applicable to the general case but does not share the disadvantages of the DFT. With the same discretely sampled Gaussian bunch profile as input, the resulting electric field pulse is shown as circles in Fig. 1. Notice that it closely follows the shape of the analytic result, even for times exceeding the duration of input bunch profile. Moreover, the peak field is only off by about 1%.

SYNCHROTRON- AND TRANSITION RADIATION

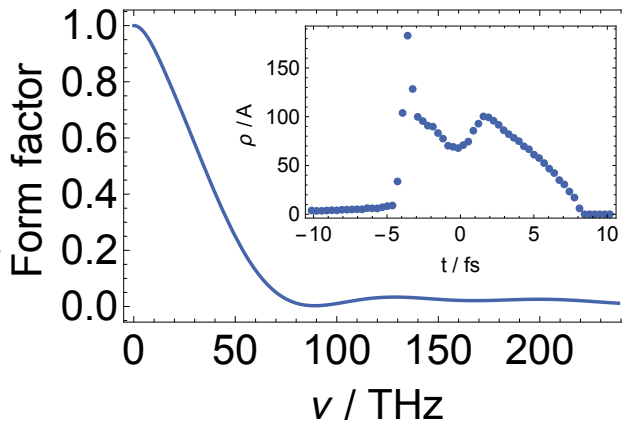


Figure 2: Form factor and (inset) longitudinal profile of the 1 pC bunch used in this paper. This simulated bunch profile [5] has an rms-bunch length of $\sigma_{\text{rms}} \sim 5$ fs, resulting in a form factor with a dominant component extending to about 50 THz, while the substructure leads to spectral content at frequencies above 130 THz.

In this section, we employ our algorithm to compute the electric field resulting from the emission of coherent SR (CSR) and TR (CTR). The simulated bunch profile has an rms-bunch length of $\sigma_{\text{rms}} \sim 5$ fs [5], and is shown in Fig. 2 together with the corresponding form factor $F(\omega) \equiv |\rho(\tilde{\omega})|^2$. Due to the ultra-short bunch length, the main part of the form factor extends up to 50 THz.

We define the single particle field $\tilde{E}_0(\omega)$ by

$$\tilde{E}_0(\omega) \equiv \sqrt{\frac{1}{2\epsilon_0 c} \frac{dI_{\text{ap}}}{d\omega}}, \quad (2)$$

where $dI/d\omega$ denotes the spectrum and the index "ap" implies that it has been obtained by integrating over the detector

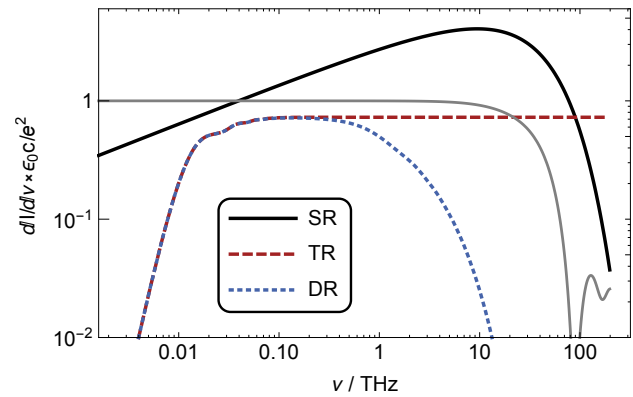


Figure 3: Single particle spectra of SR, TR, and DR (hole radius 0.5 mm) according to Eq. (3) and Eq. (4), respectively. The finite screen size acts as a low-frequency cut-off for both TR and DR. The finite hole radius leads to a high-frequency cut-off for DR, whereas TR becomes frequency independent. Notice that the form factor (thin gray line) only starts to drop for frequencies above 10 THz.

aperture. The synchrotron radiation is given by [6]

$$\frac{dI_{\text{SR,ap}}}{d\omega} = \frac{e^2 \sqrt{3}}{\epsilon_0 c 4\pi} \gamma S(\omega/\omega_c) \frac{\phi_{\text{ap}}}{2\pi}, \quad (3)$$

and ϕ_{ap} denotes the angular horizontal aperture². For diffraction radiation we use [7]

$$\frac{dI_{\text{DR,ap}}}{d\omega} = \int_{\text{ap}} \frac{dI_{\text{GF}}}{d\omega d\Omega} [T(\omega b, \theta) - T(\omega a, \theta)]^2 d\Omega. \quad (4)$$

Here, $dI_{\text{GF}}/d\omega d\Omega$ denotes the uniform Ginzburg-Frank spectrum and the functions T take the finite screen size a and the central hole radius b into account, for details consult [7]. For vanishing hole radius, i.e. $b = 0$, $T = 1$ and Eq. (4) reduces to the TR spectrum. The parameters used for the following plots are given in Table 1.

Table 1: Parameters used for Calculations

Quantity	Value
Electron energy	41 MeV
Bunch charge	1 pC
SR critical frequency ω_c (ν_c)	$2.1 \times 10^{14} \text{ s}^{-1}$ (33 THz)
Aperture angle ϕ_{ap}	0.4 rad
TR screen radius a	74 mm
DR hole radius b	0.5 mm

Figure 3 shows the spectra for SR, DR, and TR according to the equations above. The SR spectrum displays the well-known shape and peaks at about 11 THz. Both DR and TR spectra are affected by the low-frequency cut-off due to the finite screen size. The finite hole radius introduces a high-frequency cut-off for DR, whereas the TR spectrum becomes

² We assume that the vertical aperture is large enough to not significantly affect the spectrum.

frequency independent. While the peak intensity of SR is about ten times higher than that of TR, the SR spectrum decreases exponentially for frequencies larger than about 50 THz.

Using the SR and TR spectra from Eq. (3) and Eq. (4), we compute the corresponding \vec{E}_0 from Eq. (2). Next, the convolution in Eq. (1) is computed with the help of our own semi-analytic algorithm [2].

DISCUSSION

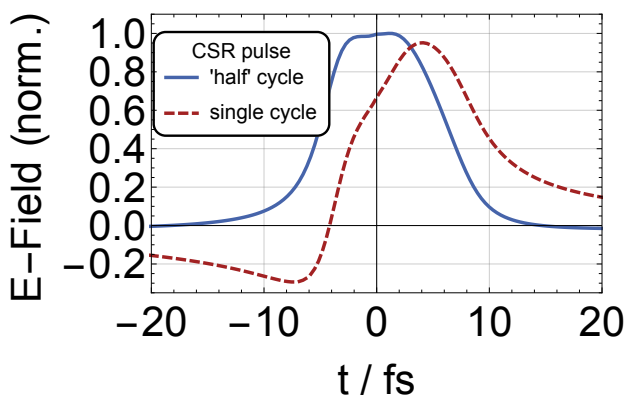


Figure 4: Electric field of the SR-pulse relative to the "half" cycle peak field, calculated with the algorithm presented in [2]. The "half" cycle pulse shape only roughly follows the bunch profile (inset in Fig. 2), because the SR spectrum suppresses the frequencies corresponding to small time scales.

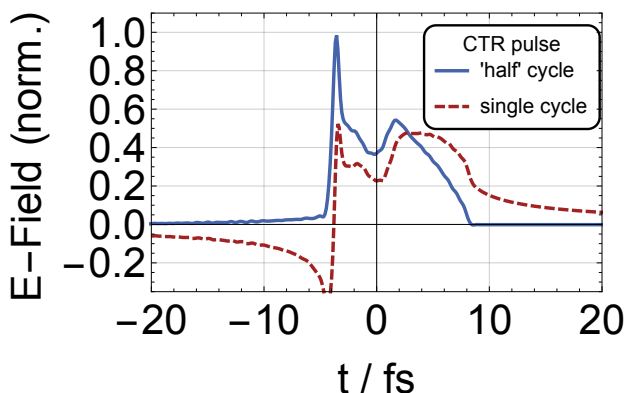


Figure 5: Electric field of the TR-pulse relative to the SR "half" cycle peak field, calculated with the algorithm presented in [2]. Since the TR-spectrum is almost flat, the "half" cycle pulse very closely follows the bunch profile (inset in Fig. 2).

Figures 4 and 5 show the electric fields of an SR and TR pulse, respectively. All fields are normalized w.r.t. the peak field of the SR "half" cycle pulse. For SR, the critical frequency ω_c coincidentally is similar to the inverse bunch length. This implies that both the single particle field \vec{E}_0 and the form factor start to decrease above the same frequency. As a result, large frequencies, corresponding to small bunch

substructure, become suppressed. Consequently, the substructure of the bunch profile gets "washed out", and the "half" cycle pulse in Fig. 4 only reflects the large-scale bunch structure.

Contrary to the SR spectrum, the TR spectrum is almost flat (see Fig. 3). Hence, \vec{E}_0 is constant to a good approximation and can be pulled out of the integral in Eq. (1a), which then turns into the inverse Fourier transform of the Fourier transform of the bunch profile. The resulting TR "half" cycle pulse, thus, very closely follows the bunch profile, see Fig. 5, because the TR spectrum has a high frequency cutoff much higher than the critical frequency for the SR spectrum. A close inspection of the tails at large times show that they are indeed negative, so that the integral over all times still vanishes, as discussed above.

When comparing the peak fields for the SR and TR pulses, we see that the peak field of TR is similar to that of SR, even though the peak intensity of SR is ten times as large. The reason for this is that the SR spectrum decreases exponentially for frequencies above 10 THz. On the other hand, the TR spectrum is almost flat and, thus, the coherent spectrum receives a non-negligible contribution also from frequencies above 130 THz arising from the sharp peak of bunch profile (see Fig. 2). Roughly, the CSR spectrum has a ten times higher peak intensity but a bandwidth which is ten times less compared to the CTR spectrum, and, as a result, the electric peak fields are of comparable magnitude. Finally, decreasing the bunch length further would not lead to a change in the SR pulse, because it is already limited by SR spectrum.

SUMMARY

We applied our semi-analytical method for calculating the electric field of a coherent THz radiation pulse [2] to an ultra-short bunch simulated for FLUTE [5]. Since the critical frequency limits the CSR, the resulting pulse shape does not follow the bunch shape. However, since the spectrum of TR is almost frequency independent, the resulting pulse shape closely follows the bunch profile. As a result, the peak electric fields of both radiation types are nearly equal. Consequently, tailored THz pulses are best produced by using TR from appropriately prepared electron bunches.

REFERENCES

- [1] M.J. Nasse et al., Rev. of Sci. Instrum. **84**, 022705 (2013).
- [2] M. Schwarz et al., MOPRO067, Proc. IPAC2014, Dresden, Germany.
- [3] M. Schwarz et al., Phys. Rev. ST Accel. Beams **17**, 050701 (2014).
- [4] K.-J. Kim et al., Phys. Rev. Lett. **84**, p. 3210 (2000).
- [5] M.J. Nasse et al., TUPWA042, Proc. IPAC2015, Richmond, USA.
- [6] H. Wiedemann, Particle Accelerator Physics, ISBN 978-3-540-49043-2, Springer (2007).
- [7] S. Casalbuoni et al., TESLA-Report 2005-05 (2005).